

# Dynamics of Microglia in the Developing Rat Brain

ISHAR DALMAU,<sup>1,2</sup> JOSÉ MIGUEL VELA,<sup>1</sup> BERTA GONZÁLEZ,<sup>1</sup> BENTE FINSEN,<sup>2</sup>  
AND BERNARDO CASTELLANO<sup>1\*</sup>

<sup>1</sup>Department of Histology, Faculty of Medicine, Autonomous University of Barcelona,  
E-08193-Bellaterra, Barcelona, Spain

<sup>2</sup>Department of Anatomy and Neurobiology, University of Southern Denmark,  
DK-5000 Odense, Denmark

---

---

## ABSTRACT

Entrance of mesodermal precursors into the developing CNS is the most well-accepted origin of microglia. However, the contribution of proliferation and death of recruited microglial precursors to the final microglial cell population remains to be elucidated. To investigate microglial proliferation and apoptosis during development, we combined proliferating cell nuclear antigen (PCNA) immunohistochemistry, *in situ* detection of nuclear DNA fragmentation (TUNEL), and caspase-3 immunohistochemistry with tomato lectin histochemistry, a selective microglial marker. The study was carried out in Wistar rats from embryonic day (E) 16 to postnatal day (P) 18 in cerebral cortex, subcortical white matter, and hippocampus. Proliferating microglial cells were found at all ages in the three brain regions and represented a significant fraction of the total microglial cell population. The percentage of microglia expressing PCNA progressively increased from the embryonic period (25–51% at E16) to a maximum at P9, when the great majority of microglia expressed PCNA (92–99%) in all the brain regions analyzed. In spite of the remarkable proliferation and expansion of the microglial population with time, the density of microglia remained quite constant in most brain regions because of the considerable growth of the brain during late prenatal and early postnatal periods. In contrast, apoptosis of microglia was detected only at certain times and was restricted to some amoeboid cells in white matter and primitive ramified cells in gray matter, representing a small fraction of the microglial population. Therefore, our results point to proliferation of microglial precursors in the developing brain as a physiological mechanism contributing to the acquisition of the adult microglial cell population. In contrast, microglial apoptosis occurs only locally at certain developmental stages and thus seems less crucial for the establishment of the final density of microglia. *J. Comp. Neurol.* 458:144–157, 2003. © 2003 Wiley-Liss, Inc.

**Indexing terms:** proliferation; proliferating cell nuclear antigen; apoptosis; DNA fragmentation; caspase-3; phagocytosis

---

---

The ontogenesis of microglia is still a matter of controversy. A neuroectodermic origin is supported by some studies (Hao et al., 1991; Fedoroff et al., 1997), but the mesodermal nature of microglia from cells of the hematopoietic lineage has been and is, at present, the most well-accepted view (Del Río Hortega, 1932; for reviews see Cuadros and Navascués, 1998; Kaur et al., 2001). In this sense, three hematopoietic cell-derived precursors, at least, have been proposed for the origin of microglia: 1) early macrophages, 2) circulating monocytes, and 3) specific hematopoietic precursors (see Cuadros and Navascués, 2001). Three routes have also been described for the invasion of the immature CNS by microglial precursors: 1) the parenchymal vascular network, 2) the surrounding meninges, and 3) the cerebral ventricles (see Cuadros and Navascués, 1998). Immigration of microglial precursors

into the developing CNS occurs during the late embryonic and early postnatal periods (Perry et al., 1985; Ashwell,

---

Grant sponsor: Marie Curie Individual Fellowship (ID), European Commission; Grant sponsor: Spanish Ministry of Science and Technology; Grant number: DGES-PB98-0892; Grant sponsor: Fundació "la Caixa," Spain; Grant number: "la Caixa" 00/074-00; Grant sponsor: the Lundbeck Foundation, Denmark; Grant sponsor: the Danish MRC.

\*Correspondence to: Bernardo Castellano, Departament de Biologia Cel·lular, de Fisiologia i d'Immunologia, Unitat d'Histologia, Torre M-5, Facultat de Medicina, Universitat Autònoma de Barcelona, E-08193 Bellaterra, Barcelona, Spain. E-mail: bernardo.castellano@uab.es

Received 11 July 2002; Revised 27 September 2002; Accepted 14 November 2002

DOI 10.1002/cne.10572

Published online the week of February 10, 2003 in Wiley InterScience (www.interscience.wiley.com).

1991; Milligan et al., 1991; Navascués et al., 1996; Dalmau et al., 1998a), and this influx of cells, which gradually increase in number and transform into mature ramified cells, is considered the basis for acquisition of the adult microglial cell population. However, similarly to what occurs with neurons and macroglial cells, the balance between proliferation and death could also contribute to the establishment of the normal density of microglia in the mature CNS.

Proliferation of neuronal and macroglial cell precursors prior to their differentiation into mature cells is a common phenomenon occurring during normal CNS development (Jacobson, 1991a,b). Periods with high mitotic rates coincide with major morphogenetic events (Jacobson, 1991a), and it has been suggested that cell division of progenitor cells depends on both their intrinsic characteristics and their response to signals provided by surrounding cells (Ross, 1996). The ability of microglia to proliferate has also been shown, being an important part of their response to the CNS injury that occurs in a broad diversity of pathological circumstances, such as lesions, infections, ischemia, and autoimmune and neurodegenerative diseases (for reviews see Kreutzberg, 1996; Streit et al., 1999). In addition, several mitogens have been reported to promote proliferation of cultured microglia (Frei et al., 1986; Giulian and Ingeman, 1988; Ganter et al., 1992; Sawada et al., 1995; Kloss et al., 1997; Luizzi et al., 1999). Similarly, both *in vitro* and *in vivo* studies have demonstrated that microglial precursors found in the developing CNS are able to proliferate (Imamoto and Leblond, 1978; Dalmau, 1998; Alliot et al., 1999; Marín-Teva et al., 1999a), but the spatiotemporal pattern of microglial proliferation during development remains to be elucidated. Therefore, not only entrance but also proliferation of recruited microglial precursors may be an inherent mechanism contributing to normal microglial homing.

Together with cell proliferation, cell death, so-called programmed cell death, is a common phenomenon that takes place in the developing CNS (for reviews see D'Mello, 1998; Roth and D'Sa, 2001), creating the balance between cellular death and proliferation essential for the normal maturation of the nervous tissue (Ross, 1996; Sommer and Rao, 2002). Large numbers of neurons die by apoptosis during normal CNS development (Cowan et al., 1984; Oppenheim, 1991; Ferrer et al., 1994), and death of macroglial cells has also been reported at different developmental stages (Raff et al., 1993; Soriano et al., 1993; Krueger et al., 1995). In various CNS pathologies microglia also undergo apoptosis (Nguyen et al., 1994; Lassmann et al., 1995; Adamson et al., 1996; Vela et al., 2002). Furthermore, microglial death can be caused by alterations in purines (Ogata and Shubert, 1996), and cytokines as well as the deprivation of various colony-stimulating factors (Yang et al., 2002) (Tomozawa et al., 1996). However, naturally occurring cell death of microglia in the developing CNS has been reported only for the postnatal spinal cord white matter (De Louw et al., 2002).

The aim of this study was to investigate the dynamics of proliferation and apoptosis of microglia in the developing rat brain during the prenatal (E16–E21) and postnatal (P0–P18) periods. Microglial proliferation was assessed by combining immunohistochemical detection of the proliferating cell nuclear antigen (PCNA) and tomato lectin histochemistry as a microglial marker. Double labeling combining immunohistochemical detection of active caspase-3

or terminal transferase mediated d-UTP nick end-labeling (TUNEL) histochemistry with the microglial marker was carried out to visualize microglial apoptosis. Here we show that proliferation of resident microglia represents a major source of microglia in the developing brain and provide evidence for caspase-3 activation and nuclear DNA fragmentation associated with microglia in the immature CNS.

## MATERIALS AND METHODS

### Experimental animals

The experimental material consisted of embryos and pups of the Wistar rat strain whose ages ranged from embryonic day 16 (E16) to postnatal day 18 (P18). Three animals, at least, of each age (E16, E18, E21, P0, P6, P9, and P18) were used. All efforts were made to minimize animal pain and distress. Experimental animal work was conducted in compliance with Spanish legislation and according to the European Union directives on this subject. Protocols were approved by the animal care committee of the Autonomous University of Barcelona, Spain.

### Preparation of sections

Pregnant rats were anesthetized with sodium pentobarbital (50 mg/kg body weight), and the fetuses were delivered by cesarean section. Embryonic brains were removed and fixed for 4 hours at room temperature (RT) with Bouin's fluid (75 ml saturated picric acid in distilled water, 25 ml formalin, and 5 ml glacial acetic acid). Postnatal animals, under pentobarbital overdose anesthesia, were perfused through the left ventricle with Bouin's fluid for 5 minutes and the brains dissected out and immersed for an additional 3 hours at room temperature (RT) in the same fixative. Then, embryonic and postnatal brains were dehydrated and embedded in paraffin. Coronal sections 10  $\mu$ m thick were obtained with the aid of a microtome, serially collected, and mounted on glass slides pretreated with 1:10 poly-L-lysine solution (Sigma, St. Louis, MO). Sections were then dewaxed, hydrated, and processed for the different techniques.

### Immunocytochemical reaction for PCNA

Sections were rinsed for 3  $\times$  5 minutes in TBS (0.05 M Trizma base containing 150 mM of NaCl), pH 7.4; treated for 10 minutes with 2% H<sub>2</sub>O<sub>2</sub> in 100% methanol to block endogenous peroxidase; and rinsed again for 3  $\times$  5 minutes in TBS and 3  $\times$  5 minutes in TBS with 0.1% Triton X-100 (TBS-T). Sections were then placed for 30 minutes at RT in blocking buffer (BB) solution containing 10% fetal bovine serum in TBS-T and incubated overnight at 4°C with the primary mouse monoclonal anti-human PCNA antibody (clone PC10; Dako, Carpinteria, CA) diluted 1:100 in BB. After three 5 minute rinses in TBS-T, sections were incubated for 60 minutes at RT with anti-mouse IgG biotinylated antibody (Amersham, Arlington Heights, IL) in a 1:200 dilution in BB, rinsed again, and incubated for 60 minutes at RT with a 1:600 dilution of avidin-peroxidase (Sigma) in BB. After three 5 minute rinses in TBS, the peroxidase reaction was visualized by transferring the sections for 5 minutes to 100 ml of 0.05 M Trizma base (TB), pH 7.4, containing 50 mg 3,3'-diaminobenzidine (DAB; Sigma), 4 ml 1% ammonium nickel sulfate, 5 ml 1% cobalt chloride, and 66  $\mu$ l H<sub>2</sub>O<sub>2</sub>.

Finally, sections were rinsed, dehydrated in graded ethanol, cleared in xylene, and coverslipped in DPX mounting medium. As a negative control for immunocytochemical staining, the primary antibody was omitted in one section per animal for each age.

### In situ labeling of nuclear DNA fragmentation: the TUNEL method

The TUNEL technique was carried out in accordance with the method of Gavrieli et al. (1992). Sections were placed for 5 minutes in 10 mM Tris-HCl, pH 8; treated for 15 minutes at RT with proteinase K (Boehringer Mannheim, Indianapolis, IN) diluted to 20  $\mu\text{g/ml}$  in Tris-HCl; and rinsed for  $4 \times 2$  minutes in double-distilled water (DDW). The endogenous peroxidase was blocked, and sections were then rinsed; transferred for 10 minutes to reaction buffer (30 mM Tris-HCl, 140 mM sodium cacodylate, 1 mM cobalt chloride), pH 7.2; and incubated in a moist chamber for 25 minutes at 37°C in reaction buffer containing 0.3 U/ $\mu\text{l}$  terminal deoxynucleotidyl transferase (Boehringer Mannheim) and 20  $\mu\text{M}$  biotinylated 16-dUTP (Boehringer Mannheim). The enzymatic reaction was stopped by rinsing twice for 10 minutes in saline sodium citrate buffer (300 mM sodium chloride, 30 mM sodium citrate). After two 2 minute rinses in DDW, sections were placed for 5 minutes in TBS and treated for 20 minutes with BB. The sections were then incubated for 60 minutes at RT with a 1:600 dilution of avidin-peroxidase in BB and rinsed again. The peroxidase reaction was performed as described above for PCNA immunocytochemistry. Finally, sections were dehydrated, cleared in xylene, and coverslipped in DPX. As a negative control, one section per animal from each age was incubated in a medium lacking either the enzyme or the biotinylated substrate.

### Immunohistochemical reaction for caspase-3

After blocking of endogenous peroxidase, sections were rinsed for  $3 \times 10$  minutes with TBS; pretreated for antigen retrieval with 10 mM citrate buffer, pH 6.0, for 20 minutes; and rinsed again for  $3 \times 10$  minutes with TBS and  $3 \times 10$  minutes with TBS-T. After treatment for 20 minutes at RT with BB, sections were incubated overnight at 4°C with 1:50 rabbit anticleaved caspase-3 (D175) polyclonal antibody (Cell Signalling). Sections were then rinsed for  $3 \times 10$  minutes with TBS-T, incubated at RT for 1 hour in 1:200 anti-rabbit IgG biotinylated antibody (Amersham), rinsed for  $3 \times 10$  minutes in TBS-T, and incubated for 1 hour at RT with a 1:600 dilution of avidin-peroxidase in BB. After being rinsed, the peroxidase reaction product was visualized by incubating the sections in 100 ml TB containing 50 mg DAB and 33  $\mu\text{l}$   $\text{H}_2\text{O}_2$ . Finally, sections were dehydrated in graded ethanols, cleared in xylene, and coverslipped in DPX mountant medium (Bancroft and Stevens, 1996). As a negative control for immunocytochemical staining, the primary antibody was omitted in one section per animal for each age.

### Double-labeling techniques

To detect proliferating microglia, paraffin sections were processed for double labeling (Vela et al., 1997) by sequentially combining PCNA immunostaining and tomato lectin (TL) histochemistry. Simultaneous demonstration of apoptotic microglia was achieved through sequential combination of TUNEL (Vela et al., 1996) or caspase-3 immu-

nohistochemistry and TL histochemistry. Tomato lectin is a lectin obtained from *Lycopersicon esculentum* (tomato), which is specific for oligomers of poly-N-acetyllactosamine containing three repeating Gal ( $\beta$ 1-4)GlcNAc ( $\beta$ 1-3)-disaccharides that specifically bind poly-N-acetyl lactosamine residues (glcNAc)<sub>3</sub> (Zhu and Laine, 1989). Biotinylated TL is commonly used as a histochemical microglial marker in both the prenatal CNS (Dalmau et al., 1997b) and the postnatal CNS (Acarin et al., 1994) as well as in the adult (Acarin et al., 1994). Two types of controls were carried out. First, some sections were incubated only with avidin-peroxidase. Second, the specificity of TL was confirmed by incubating some sections in a 0.1 M solution of N-acetyl lactosamine (Sigma A-7791) for 30 minutes before incubation with the biotinylated lectin in a sugar solution (Acarin et al., 1994).

**PCNA/TL and TUNEL/TL double staining.** PCNA- and TUNEL-stained sections were rinsed for  $3 \times 5$  minutes in TBS, and peroxidase activity was blocked with 2%  $\text{H}_2\text{O}_2$  in 100% methanol for 10 minutes at RT. After three 10 minute rinses in TBS-T, the sections were incubated overnight at 4°C with the biotinylated TL (*Lycopersicon esculentum*; Sigma) diluted to 15  $\mu\text{g/ml}$  in TBS-T. Sections were then rinsed for  $3 \times 15$  minutes in TBS-T, incubated for 1 hour at RT with a 1:600 dilution of avidin-peroxidase in TBS-T, and rinsed again. The peroxidase reaction was visualized by incubating the sections in 100 ml of TB containing 50 mg DAB and 33  $\mu\text{l}$   $\text{H}_2\text{O}_2$  for 5 minutes. Most sections were counterstained with Harris's hematoxylin. Finally, sections were dehydrated in graded ethanols, cleared in xylene, and coverslipped in DPX mounting medium (Bancroft and Stevens, 1996).

**Double caspase-3/TL immunofluorescence.** For simultaneous visualization of caspase-3 and microglia, some sections from each animal and for each age were immunostained for caspase-3 as described previously but using rabbit anticleaved caspase-3 (D175) polyclonal antibody and a 1:1,000 dilution of Cy3-conjugated anti-rabbit IgG (Amersham) as secondary antibody. Double labeling for TL was visualized using the biotinylated TL and 1:1,000 Cy2-conjugated avidin (Amersham). Finally, sections were coverslipped with Glycergel mounting media (Dako).

### Quantification and statistical analysis

The quantitative study was carried out to determine numbers and densities of microglia (see Fig. 2, Table 1), proliferating microglia (see Fig. 2, Table 1), and apoptotic microglia (Table 1). In addition, the density of phagocytosing microglia (Table 2) throughout all ages was quantified. The brain regions analyzed were cerebral cortex, subcortical white matter (corpus callosum and external capsule), and hippocampus (Ammon's horn, dentate gyrus, and fimbria). Values for the subcortical white matter at E16 were not given because of the difficulties in delineating the area at this age (Altman and Bayer, 1995). Cell counting in Ammon's horn on day E16 includes not only this subregion but also the developing dentate gyrus and the fimbria, because none of these structures are clearly distinguishable at this early age (Altman and Bayer, 1995). In total, three animals per age were used for this purpose. Number of cells and cell density (number of cells per square millimeter) values were obtained by counting cells in six randomly selected coronal sections at the central/midposterior level per animal and for each brain

TABLE 1. PCNA- or TUNEL-Labeled Microglial Cells in the Developing Rat Brain<sup>1</sup>

|                                 | Number of cells           |                                |                 | Density (cells/mm <sup>2</sup> ) |                          |                 |
|---------------------------------|---------------------------|--------------------------------|-----------------|----------------------------------|--------------------------|-----------------|
|                                 | Microglia                 | Microglia-PCNA (%)             | Microglia-TUNEL | Microglia                        | Microglia-PCNA           | Microglia-TUNEL |
| <b>Gray matter</b>              |                           |                                |                 |                                  |                          |                 |
| <b>Cerebral cortex</b>          |                           |                                |                 |                                  |                          |                 |
| E16                             | 8.8 ± 0.6                 | 4.5 ± 0.6 <sup>2</sup> (51)    | 0               | 13.0 ± 0.9                       | 6.6 ± 0.9                | 0               |
| E18                             | 21.6 ± 2.4 <sup>2</sup>   | 11.8 ± 0.9 <sup>2</sup> (55)   | 0               | 14.7 ± 1.5                       | 8.0 ± 0.6                | 0               |
| E21                             | 34.8 ± 1.4 <sup>2</sup>   | 18.8 ± 0.4 <sup>2</sup> (54)   | 0               | 13.3 ± 1.2                       | 7.1 ± 0.4                | 0               |
| P0                              | 63.3 ± 2.8 <sup>2</sup>   | 47.8 ± 2.9 <sup>2</sup> (75)   | 0               | 17.0 ± 0.8                       | 12.8 ± 0.7 <sup>2</sup>  | 0               |
| P6                              | 113.3 ± 1.5 <sup>2</sup>  | 109.3 ± 1.9 <sup>2</sup> (96)  | 0               | 15.5 ± 0.5                       | 14.9 ± 0.5               | 0               |
| P9                              | 432.1 ± 20.8 <sup>2</sup> | 426.5 ± 20.1 <sup>2</sup> (99) | 0               | 51.8 ± 2.2 <sup>2</sup>          | 51.1 ± 2.1 <sup>2</sup>  | 0               |
| P18                             | 641.0 ± 1.3 <sup>2</sup>  | 273.0 ± 1.3 <sup>2</sup> (43)  | 0               | 60.4 ± 0.1 <sup>2</sup>          | 25.7 ± 0.1 <sup>2</sup>  | 0               |
| <b>Ammon's horn</b>             |                           |                                |                 |                                  |                          |                 |
| E16                             | 11.6 ± 1.6                | 4.6 ± 0.9 (39)                 | 0               | 50.1 ± 5.9                       | 19.8 ± 3.7               | 0               |
| E18                             | 11.0 ± 1                  | 5.0 ± 0.5 (45)                 | 0               | 37.2 ± 2.4                       | 16.7 ± 0.6               | 0               |
| E21                             | 30.5 ± 3.9 <sup>2</sup>   | 10.1 ± 1 <sup>2</sup> (33)     | 0               | 44.9 ± 4.7                       | 15.0 ± 1.3               | 0               |
| P0                              | 43.0 ± 3 <sup>2</sup>     | 34.0 ± 1.7 <sup>2</sup> (79)   | 0               | 49.8 ± 3.4                       | 39.4 ± 1.9 <sup>2</sup>  | 0               |
| P6                              | 88.0 ± 1 <sup>2</sup>     | 83.6 ± 0.5 <sup>2</sup> (95)   | 0.2 ± 0.2       | 55.4 ± 3.9                       | 52.6 ± 3.7 <sup>2</sup>  | 1.2 ± 1.2       |
| P9                              | 131.5 ± 4.2 <sup>2</sup>  | 124.8 ± 4.2 <sup>2</sup> (95)  | 0.7 ± 0.4       | 64.1 ± 1.8                       | 60.8 ± 1.7               | 3.2 ± 2.1       |
| P18                             | 226.3 ± 2.3 <sup>2</sup>  | 30.0 ± 0.7 <sup>2</sup> (13)   | 0               | 74.2 ± 0.7 <sup>2</sup>          | 9.8 ± 0.2 <sup>2</sup>   | 0               |
| <b>Dentate gyrus</b>            |                           |                                |                 |                                  |                          |                 |
| E16                             | —                         | —                              | —               | —                                | —                        | —               |
| E18                             | 0.1 ± 0.1                 | 0                              | 0               | 6.2 ± 6.2                        | 0                        | 0               |
| E21                             | 1.6 ± 0.2 <sup>2</sup>    | 0.4 ± 0.2 (25)                 | 0               | 12.3 ± 1.3                       | 2.7 ± 1.6                | 0               |
| P0                              | 3.8 ± 0.5 <sup>2</sup>    | 1.5 ± 0.2 <sup>2</sup> (39)    | 0               | 28.9 ± 4.5 <sup>2</sup>          | 11.4 ± 1.8 <sup>2</sup>  | 0               |
| P6                              | 17.0 ± 1.4 <sup>2</sup>   | 16.0 ± 1 <sup>2</sup> (94)     | 0               | 37.5 ± 4.3                       | 35.3 ± 3.6 <sup>2</sup>  | 0               |
| P9                              | 54.3 ± 4.8 <sup>2</sup>   | 51.6 ± 4.2 <sup>2</sup> (95)   | 0               | 75.5 ± 8.4 <sup>2</sup>          | 71.7 ± 7.4 <sup>2</sup>  | 0               |
| P18                             | 69.6 ± 0.9 <sup>2</sup>   | 20.0 ± 1 <sup>2</sup> (29)     | 0               | 50.2 ± 0.6 <sup>2</sup>          | 14.4 ± 0.7 <sup>2</sup>  | 0               |
| <b>White matter</b>             |                           |                                |                 |                                  |                          |                 |
| <b>Subcortical white matter</b> |                           |                                |                 |                                  |                          |                 |
| E16                             | —                         | —                              | 0               | —                                | —                        | 0               |
| E18                             | 59.0 ± 3                  | 16.6 ± 0.8 (28)                | 0               | 260.1 ± 10.5                     | 73.5 ± 3.4               | 0               |
| E21                             | 65.6 ± 2.3                | 22.5 ± 1.3 <sup>2</sup> (34)   | 0.2 ± 0.2       | 81.1 ± 4.7 <sup>2</sup>          | 27.9 ± 2.4 <sup>2</sup>  | 0.1 ± 0.1       |
| P0                              | 103.1 ± 7.4 <sup>2</sup>  | 65.6 ± 3.7 <sup>2</sup> (64)   | 0               | 104.1 ± 7.50                     | 66.2 ± 3.7 <sup>2</sup>  | 0               |
| P6                              | 66.0 ± 3.5 <sup>2</sup>   | 58.0 ± 3.8 (88)                | 0               | 62.0 ± 4.5 <sup>2</sup>          | 54.6 ± 4.6               | 0               |
| P9                              | 228.6 ± 4.1 <sup>2</sup>  | 218.5 ± 5.9 <sup>2</sup> (95)  | 0               | 215.2 ± 5.1 <sup>2</sup>         | 205.5 ± 5.4 <sup>2</sup> | 0               |
| P18                             | 221.8 ± 0.9               | 70.3 ± 0.4 <sup>2</sup> (32)   | 0               | 116.8 ± 0.4 <sup>2</sup>         | 37.0 ± 0.2 <sup>2</sup>  | 0               |
| <b>Fimbria</b>                  |                           |                                |                 |                                  |                          |                 |
| E16                             | —                         | —                              | 0               | —                                | —                        | 0               |
| E18                             | 6.0 ± 0.4                 | 1.8 ± 0.3 (30)                 | 0.2 ± 0.2       | 104.4 ± 6.3                      | 31.3 ± 4.3               | 2.5 ± 2.5       |
| E21                             | 13.0 ± 1.3 <sup>2</sup>   | 8.0 ± 1.2 <sup>2</sup> (62)    | 0               | 102.5 ± 19.4                     | 65.0 ± 1.5 <sup>2</sup>  | 0               |
| P0                              | 17.6 ± 0.4 <sup>2</sup>   | 14.0 ± 0.5 <sup>2</sup> (79)   | 0               | 112.9 ± 2.7                      | 88.6 ± 3.3 <sup>2</sup>  | 0               |
| P6                              | 18.0 ± 0.3                | 16.0 ± 0.3 <sup>2</sup> (89)   | 0               | 66.5 ± 7.1 <sup>2</sup>          | 59.2 ± 6.4 <sup>2</sup>  | 0               |
| P9                              | 33.1 ± 0.6 <sup>2</sup>   | 30.6 ± 0.6 <sup>2</sup> (92)   | 0.2 ± 0.2       | 141.3 ± 3.3 <sup>2</sup>         | 130.6 ± 2.7 <sup>2</sup> | 0.6 ± 0.6       |
| P18                             | 32.6 ± 0.2                | 10.6 ± 0.2 <sup>2</sup> (32)   | 0               | 77.2 ± 0.4 <sup>2</sup>          | 25.2 ± 0.4 <sup>2</sup>  | 0               |

<sup>1</sup>The quantitative data are based on cell countings of 3 animals per age. Values are in means ± SEM. Microglia-PCNA, microglial cells expressing PCNA. Microglia-TUNEL, TUNEL-positive microglial cells in relation to the total of TUNEL-positive cells (Table 2).  
<sup>2</sup>Statistically significant with regard to previous age ( $P < 0.05$ ).

TABLE 2. Density of TUNEL-Positive Cells engulfed by TL-Labeled Microglial Cells<sup>1</sup>

|     | Cerebral cortex        |                              | Ammon's horn            |                               | Dentate gyrus           |                              | Subcortical white matter |                              | Fimbria                 |                              |
|-----|------------------------|------------------------------|-------------------------|-------------------------------|-------------------------|------------------------------|--------------------------|------------------------------|-------------------------|------------------------------|
|     | TUNEL                  | TUNEL/TL (%)                 | TUNEL                   | TUNEL/TL (%)                  | TUNEL                   | TUNEL/TL (%)                 | TUNEL                    | TUNEL/TL (%)                 | TUNEL                   | TUNEL/TL (%)                 |
| E16 | 6.8 ± 0.3              | 1.2 ± 0.2 (18)               | 23.6 ± 3.3              | 20.9 ± 3 (88)                 | —                       | —                            | —                        | —                            | —                       | —                            |
| E18 | 0.3 ± 0.1 <sup>2</sup> | 0.3 ± 0.1 <sup>2</sup> (100) | 5.2 ± 1.1 <sup>2</sup>  | 4.7 ± 0.9 <sup>2</sup> (91)   | 0                       | 0 (0)                        | 7.3 ± 1.4                | 6.6 ± 1 (90)                 | 79 ± 12.6               | 76.5 ± 10.2 (97)             |
| E21 | 0.7 ± 0.1 <sup>2</sup> | 0.6 ± 0.1 (90)               | 4 ± 0.3                 | 3.2 ± 0.3 (81)                | 1.4 ± 1.4 <sup>2</sup>  | 0 (0)                        | 2.8 ± 0.4 <sup>2</sup>   | 1.6 ± 0.2 <sup>2</sup> (56)  | 22.4 ± 5.5 <sup>2</sup> | 21.5 ± 6 <sup>2</sup> (96)   |
| P0  | 4.4 ± 0.2 <sup>2</sup> | 3.8 ± 0.2 <sup>2</sup> (86)  | 18.2 ± 1.8 <sup>2</sup> | 18.2 ± 1.8 <sup>2</sup> (100) | 20.4 ± 4.2 <sup>2</sup> | 19.1 ± 3.6 <sup>2</sup> (93) | 18.1 ± 2.4 <sup>2</sup>  | 17.1 ± 1.8 <sup>2</sup> (94) | 34.8 ± 5.3              | 34.8 ± 5.3 (100)             |
| P6  | 4 ± 0.3                | 3.5 ± 0.2 <sup>2</sup> (87)  | 10.6 ± 2.6              | 5.2 ± 0.7 <sup>2</sup> (49)   | 12.7 ± 2.2              | 6.9 ± 0.8 <sup>2</sup> (54)  | 26.7 ± 3.6               | 22.4 ± 1.7 (84)              | 15.3 ± 2.4 <sup>2</sup> | 11.2 ± 2.1 <sup>2</sup> (73) |
| P9  | 1.5 ± 0.9 <sup>2</sup> | 1.4 ± 0.2 <sup>2</sup> (93)  | 3.7 ± 0.6 <sup>2</sup>  | 2.7 ± 0.7 (74)                | 4.4 ± 0.5 <sup>2</sup>  | 3.2 ± 0.8 <sup>2</sup> (73)  | 16.4 ± 1 <sup>2</sup>    | 15.3 ± 1.5 <sup>2</sup> (93) | 13.5 ± 2.3              | 11.3 ± 2.3 (84)              |
| P18 | 0.6 ± 0                | 0.5 ± 0 <sup>2</sup> (83)    | 1.3 ± 0.2 <sup>2</sup>  | 1 ± 0.1 <sup>2</sup> (76)     | 2.6 ± 0.3 <sup>2</sup>  | 1.8 ± 0.4 (71)               | 5.5 ± 0.6 <sup>2</sup>   | 4.3 ± 4.8 <sup>2</sup> (79)  | 0 <sup>2</sup>          | 0 <sup>2</sup> (0)           |

<sup>1</sup>The quantitative data are based on cell countings of three animals per age. Density is expressed in cells/mm<sup>2</sup>. Values are in means ± SEM. TUNEL, TUNEL-positive cells. TUNEL/TL, TL-positive cells engulfing TUNEL-labeled cells. Percentage of TUNEL-positive cells engulfed by TL-labeled microglial cells.  
<sup>2</sup>Statistically significant with regard to previous age.

region and age. In practice, the area (square millimeters) for each brain region throughout all ages was first defined by digitizing histological sections with the aid of a video camera mounted on a Leitz microscope and interfaced to a Macintosh computer using the National Institutes of Health Image software (NIH 1.52). The cell density for each age in each brain region, based on this analysis, was calculated by dividing the total cell number by the area (square millimeters). Quantification was performed under the microscope, using a 40× objective. All cells were counted by the same person (I.D.). The criteria for count-

ing a cell were as follows: 1) TL-labeled microglia had a brownish-stained cytoplasm (with or without a cell process) surrounding a small, oval to round heterochromatic hematoxylin blue-stained nucleus; 2) PCNA-labeled microglia displayed a PCNA black-stained nucleus surrounded by a brownish TL-stained cytoplasm (with or without a cell process); 3) TUNEL-positive microglia had either a TUNEL black-stained nucleus with a surrounding brownish TL-stained cytoplasm (with or without a cell process) or a hematoxylin-stained nucleus with an intense peripheral TUNEL black labeling surrounded by a brown-

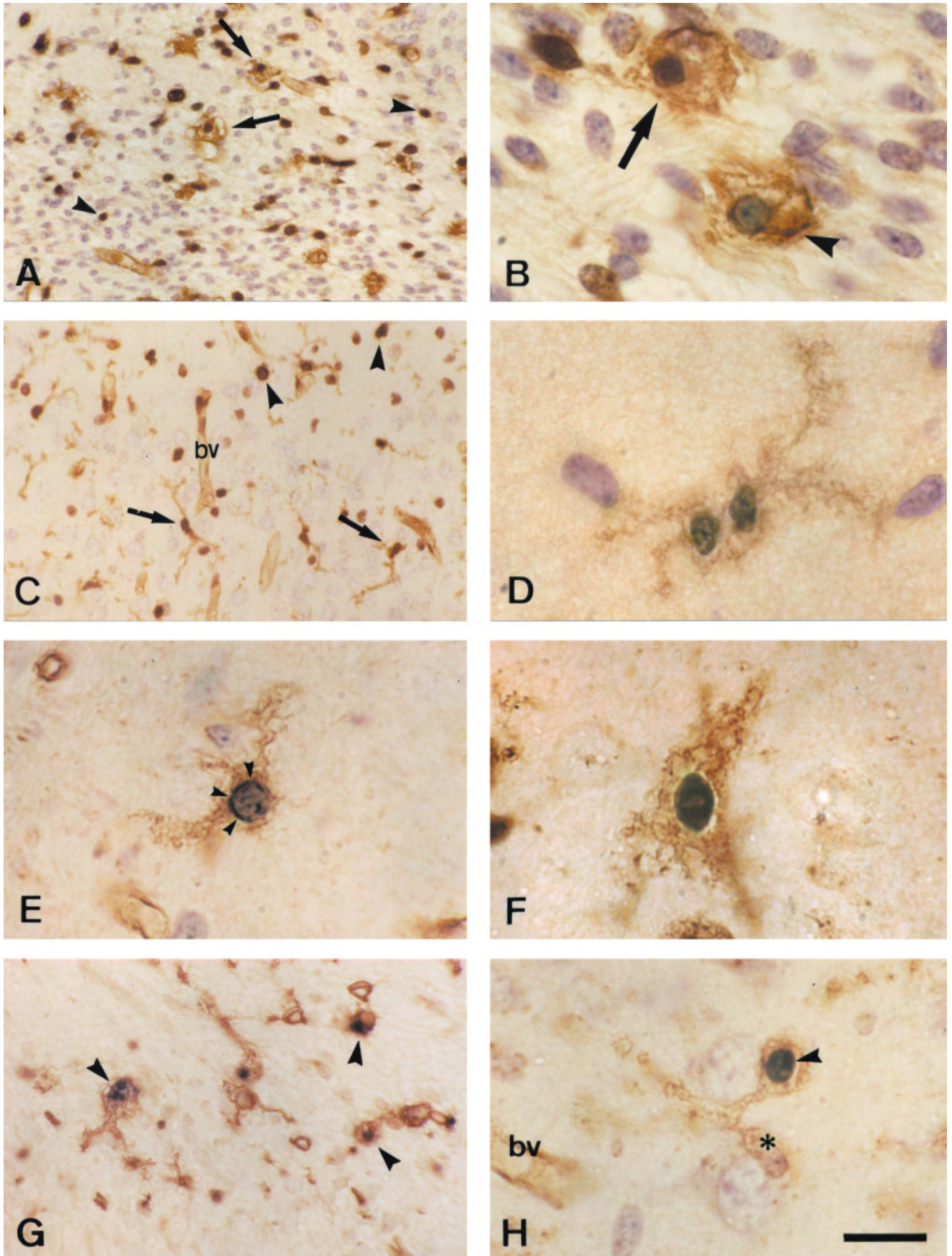


Figure 1

ish TL-stained cytoplasm (with or without a cell process); 4) TUNEL-labeled cells were distinguished as having intensely and homogeneously TUNEL-stained nuclei or a hematoxylin-stained nucleus with an intense peripheral TUNEL black labeling; and 5) phagocytosing microglia were distinguished as TL-labeled microglia showing a hematoxylin-stained heterochromatic nucleus and engulfing or containing TUNEL black-positive material in either the cytoplasm or cell processes, corresponding to apoptotic cells other than the microglial cell itself.

Analysis of variance (ANOVA) and Scheffé's test were performed at the 95% significance level. Statistical comparison was made from one age to the previous one throughout all time points for each brain region.

### Photomicrograph production

The photomicrographs shown in Figure 1 were obtained by digitizing histological sections with the aid of a video camera mounted on a Leitz microscope and interfaced to a Macintosh computer. The photomicrographs in Figure 3 were obtained with a Leitz confocal microscope interfaced to a PC computer. Final photomicrographs were generated using Adobe Photoshop 5.5.

## RESULTS

Microscopic examination of TL histochemistry in the developing rat brain revealed the presence of a heterogeneous population of cells belonging to the microglial cell lineage in the different brain structures analyzed: cerebral cortex, subcortical white matter, and hippocampal subregions Ammon's horn, dentate gyrus, and fimbria. In addition to microglia, TL also stained blood vessel endothelium, ependyma, and choroid plexus epithelium, but this labeling did not interfere with microglial identification. Sections processed as negative controls for lectin staining were devoid of specific labeling.

Three types of microglia were distinguished based on morphological features and according to our previous data (for a detailed study see Dalmau et al., 1998a): amoeboid microglia (AM), primitive ramified microglia (PRM), and mature ramified microglia (RM). The three morphologic

typologies corresponded to different steps in the maturation of microglia, and each microglial cell type showed a specific time course of appearance and distribution pattern. AM (Fig. 1A,B) were roundish cells with filopodia and pseudopodia that were first found on E16 and gradually transformed into PRM with age. PRM (Fig. 1C) were poorly ramified cells that represent intermediate forms in the differentiation process from AM to RM. PRM were first found on E18 and were the most widespread microglial cell type up to P9. RM, the mature ramified microglia, were rarely found before P9 but were the only type found in the brain from P18.

### Proliferation of microglia visualized by PCNA/TL double staining

Double PCNA/TL staining enabled us to visualize simultaneously PCNA-positive nuclei (black staining) and TL-positive microglia (brownish staining; Fig. 1A–D). AM (Fig. 1A,B) and PRM (Fig. 1C,D) accounted for the majority of PCNA-positive microglial cells, whereas RM rarely expressed PCNA. PCNA-positive AM were found mostly in the prenatal period, in both gray and white matter, although they were restricted to white matter in the postnatal period (up to P9). PCNA-positive PRM were preferentially demonstrated in the postnatal period and distributed in gray and white matter. Some TL-positive cells other than microglia (vascular endothelial cells, ependyma, and choroid plexus epithelial cells) and some non-TL-positive cells also expressed PCNA. The quantitative analysis (Fig. 2, Table 1) revealed that the number of PCNA-positive microglia increased from the prenatal period, when less than half of the microglial cell population expressed PCNA in most brain regions, reaching a maximum on P9 in all gray and white matter brain regions, when the great majority of microglia expressed PCNA: 99% in the cerebral cortex, 95% in the hippocampal regions Ammon's horn and dentate gyrus, 95% in the subcortical white matter, and 92% in the fimbria. In conclusion, although some differences between regions could be noted, a significant peak increase in the number of PCNA/TL double-stained cells was observed in most regions from P6 to P9 along with a significant reduction from P9 to P18.

### Developmental changes in the microglial cell population and cell densities

The microglial population expanded significantly from the prenatal period to the postnatal ages in both gray and white matter (Fig. 2, Table 1). However, the increase in microglial numbers showed a different dynamic when comparing different gray and white matter regions. In each region, the microglial cell population on average significantly expanded up to 2-fold when comparing one age with the previous age, with the following exceptions: 1) 2.5- to 3-fold in the cerebral cortex from E16 to E18, the Ammon's horn from E18 to E21, and the dentate gyrus from E21 to P0 and from P6 to P9; 2) around 3.5-fold from P6 to P9 in the cerebral cortex and the fimbria; and 3) around 4.5-fold in the dentate gyrus from P0 to P6. In contrast, there was a significant decrease in the microglial cell numbers of 1.5-fold only in the subcortical white matter from P0 to P6.

Despite marked increases in the number of fetal cells counted, the density of microglia (number of cells per square millimeter) remained quite constant during devel-

Fig. 1. Double-labeling technique combining TL histochemistry for the demonstration of microglia (brown staining) and PCNA immunohistochemistry (A–D) or TUNEL (E–H) staining (black staining). Sections were also counterstained with hematoxylin. A,B: Subcortical white matter on E21. Amoeboid microglial (A,B) cells often showed nuclear PCNA immunostaining (arrows) in the prenatal period, although some of them (arrowhead in B) did not colocalize PCNA staining. In A, note that PCNA expression was also found in cells other than microglia (arrowheads in A). C,D: Cerebral cortex at P9. Primitive ramified microglial cells expressing PCNA (arrows in C). Cells other than microglia also expressed PCNA (arrowheads in C). Interestingly, pairs of juxtaposed PCNA-positive microglial cells were seen (D). E: Primitive ramified microglia displaying a peripheral nuclear TUNEL staining (arrowheads) in the stratum radiatum of the hippocampus at CA1 subregion at P9. F: Microglial cell nucleus (blackish staining) showing a dark and homogenous TUNEL staining in the cerebral cortex at P0. G: Microglia engulfing TUNEL-positive cells (arrowheads) at the border between the CA1 stratum oriens and the dorsal hippocampal commissure at the day of birth. H: Primitive ramified microglia showing its own nucleus (asterisk) and engulfing a TUNEL-labeled apoptotic nucleus by means a cell process (arrowhead). bv, Blood vessel. Scale bar = 50  $\mu$ m for A,C, 15  $\mu$ m for B,D–G, 30  $\mu$ m for H.

## Gray Matter

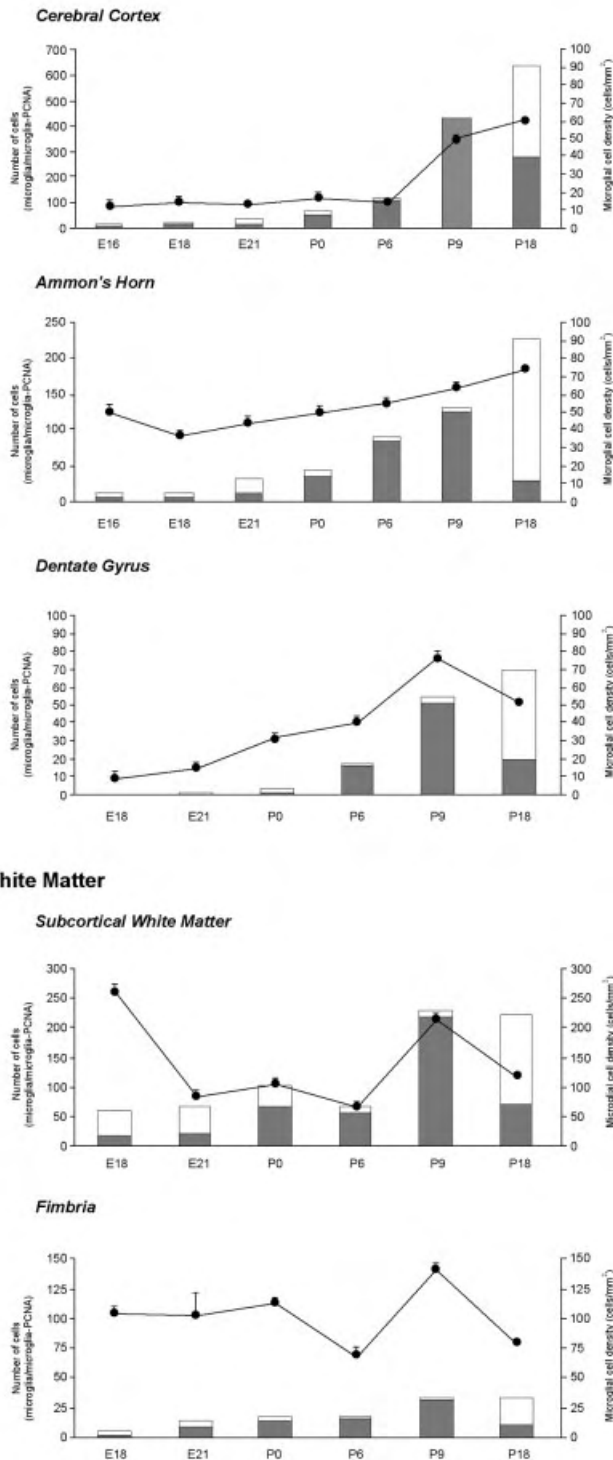


Fig. 2. Quantification of microglia in the developing rat brain. Histograms and line graphs are obtained from data in Table 1. Histograms show the number of microglial cells in each brain region and throughout the ages selected in the present study. The inferior black part of each column represents the fraction of microglia that were actively proliferating based on their double PCNA/TL staining. Line graphs represent the time course of microglial density in the different brain regions analyzed.

opment (Fig. 2, Table 1). In general, a significant increase was found only during the postnatal time, particularly P6–P9 or P9–P18, depending on the region. The microglial density was in general higher and reached its maximum earlier in white than in gray matter. In the different gray matter regions, the highest microglial densities were found on P9–P18 and were 50–75 cells/mm<sup>2</sup>, whereas, in white matter, maximal densities were found on E18 in the subcortical white matter and on P9 in the fimbria, where they were approximately 260 and 140 cells/mm<sup>2</sup>, respectively. In addition, the changes in microglial density through ages showed a different dynamic in gray and white matter. With the exception of the dentate gyrus, which showed a significant reduction in microglial cell density from P9 to P18, microglial density in the developing gray matter was characterized by a slow increase in cell density from the embryonic period throughout the postnatal period. In contrast, microglial density in white matter displayed cyclic changes, with a decrease from E18 to E21, an increase from E21 to P0, a new decrease from P0 to P6, a new increase from P6 to P9, and a final decrease from P9 to P18.

## Apoptosis of microglia visualized by DNA fragmentation and caspase-3 activation

Detection of in situ nuclear DNA fragmentation by TUNEL and expression of active, cleaved caspase-3 by immunocytochemistry are frequently used methods for visualization of apoptotic cells in tissue sections (Gavrieli et al., 1992; Gown and Willingham, 2002). Double TUNEL/TL staining allowed the simultaneous visualization of TUNEL-positive nuclei (black staining) and TL-positive microglial cells (brownish staining; Fig. 1E,F). Most TUNEL-positive cells showed an intense and homogeneous nuclear staining (Fig. 1F), but cells showing a peripheral nuclear labeling (Fig. 1E) were also observed. Microglia were frequently found close to or clustering around TUNEL-positive nuclei, but only some TUNEL-positive microglial nuclei were noted. The presence of low numbers of apoptotic microglia was also confirmed by double-fluorescence labeling combining caspase-3 immunohistochemistry (red) and TL histochemistry (green; Fig. 3A–I). The quantitative analysis (Table 1) revealed that apoptotic microglia represented a small fraction of the microglial cell population. Apoptotic microglia were mainly AM located in white matter and PRM located in gray matter. Very rarely, we observed RM showing nuclear DNA fragmentation. With regard to their temporospatial distribution, apoptotic microglia in white matter were found mainly in the fimbria on days E18 and P9 and in the subcortical white matter at E21, whereas they were observed in gray matter on days P6 and P9 in Ammon's horn. At other ages and locations, microglial cells showing positive TUNEL or caspase-3 staining were infrequently found.

## Phagocytosis by microglia

A remarkable association of TUNEL-positive (Fig. 1G,H) and caspase-3-positive cells (Fig. 3J–L) and microglia was found when examining double labeling combining TUNEL-labeling or caspase-3 immunohistochemistry with TL histochemistry. Not only amoeboid (Fig. 1G) but also ramified (Figs. 1H, 3J–L) microglial cells were found adjacent to, clustering around, engulfing, or containing TUNEL-positive cells. The quantitative analysis (Table 2)

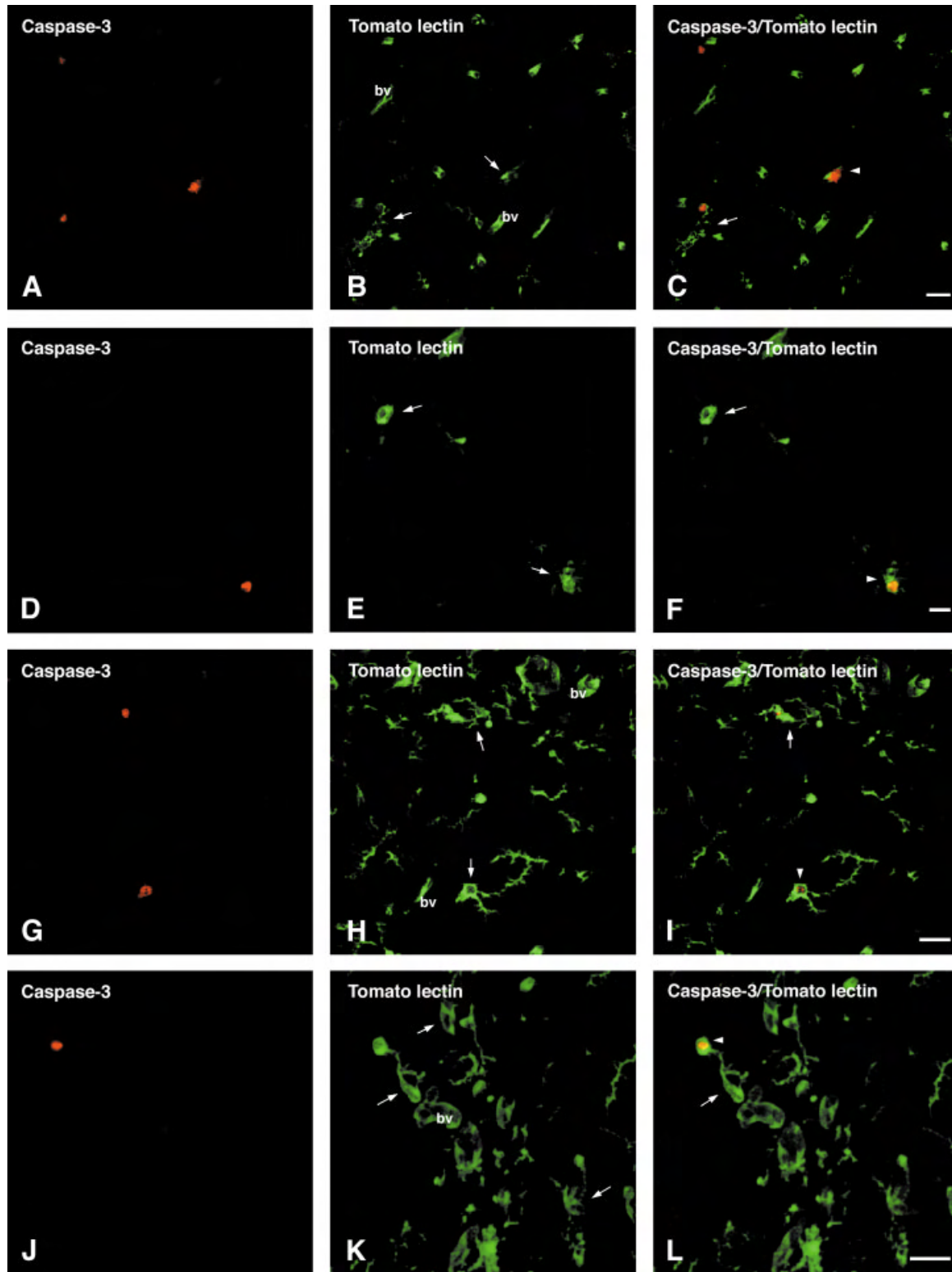


Fig. 3. Double-staining technique combining immunohistochemistry to demonstrate caspase-3 activation (red staining) and tomato lectin histochemistry for the visualization of microglia (green staining). A–I: Cerebral cortex (A–C) and hippocampus (D–I) on P6. Similarly to the detection of DNA fragmentation by TUNEL in cells of the microglial lineage, the expression of active caspase-3 (A,D,G) was investigated in this glial cell type (arrows in B,E,H), showing a colocalization of the enzyme in some cells of the microglial population (ar-

rowheads in C,F,I), although they were generally negative for this colocalization (arrows in C,F,I). J–L: Primitive ramified microglia (arrows in K and arrow in L) in the dentate gyrus at P6 are also observed engulfing caspase-3-positive cells (J and arrowhead in L) by means of a cell process, corroborating the evidence that not only ameboid but also maturing ramified microglia have the ability to phagocytose in the developing brain. bv, Blood vessel. Scale bars in C,F = 10  $\mu$ m for A–F; bars in I,L = 20  $\mu$ m for G–L.



showed that, except for a few ages and in certain brain regions, more than 70% of TUNEL-positive cells were in close association with microglia. The highest mean percentages were found in the cerebral cortex at E18, in Ammon's horn at P0, and in the fimbria at P0, when close to 100% of TUNEL-positive cells were being engulfed by TL-positive microglia.

## DISCUSSION

### Microglial proliferation and density of microglia during development

The present study demonstrates that proliferation of microglia is a remarkable event that takes place in the developing CNS, and this event contributes significantly to the establishment of normal microglial density in the mature CNS. The time course of microglial proliferation paralleled the temporal pattern of microglial differentiation: Immature AM and PRM found in the embryonic and early postnatal periods proliferated at higher levels than the mature RM found in the late postnatal period. We show here that a significant fraction of microglia proliferates during CNS development, during both prenatal and postnatal periods. The percentage of microglia expressing PCNA progressively increased with time, reaching the maximum at P9. About 50% of the microglial cell population expressed PCNA during the prenatal period, and, when at a maximum at P9, the great majority (92–99%) of microglia expressed PCNA in the gray and white matter. This means that the severalfold expansion of the microglial cell population that takes place from P6 to P9 can almost be accounted for by proliferation of resident AM and PRM cells. However, proliferation does not result in a progressive parallel increase in microglial density with time. On the contrary, insofar as the brain is an organ that experiences remarkable morphogenetic changes and undergoes significant volume expansion during development, the density of microglia remained quite constant during development. On this basis, it appears that proliferation serves not only to promote an increase in the density of microglia but more importantly to maintain a relatively constant density of cells during the maturation of the CNS. In accordance with our observations, studies by Kaur et al. (1989) of other CNS regions have also shown that the highest microglial density is found during the last part of the first week and during the second postnatal week. Similarly, a quantitative study of microglial ontogenesis in the rat corpus callosum showed a marked increase in the microglial cell density between P4 and P8 (Wu et al., 1992). In the rat pituitary, microglial proliferation peaked in both neurohypophysis and adenohypophysis on P14 (Mander and Morris, 1996).

Proliferation of microglia/macrophages in the present study was recognized by expression of PCNA (Kurki et al., 1988; Kelman, 1997) and the increase in cell numbers. However, we cannot discard the possibility that some microglial precursors entered the cell cycle and expressed PCNA without undergoing cell division, as suggested previously (Vela et al., 2002). For progression from G<sub>1</sub> to S, some factors are required (Avanzi et al., 1991; Gadbois et al., 1995), and it is accepted that some cells that become activated and enter the cell cycle may also rest quiescently in G<sub>1</sub>. G<sub>1</sub>-arrested cells express PCNA (Zölzer et al., 1994; Gadbois et al., 1995), and this may result in the appear-

ance of PCNA-immunoreactive cells without producing an increase in the number of S-phase cells (McCormick and Hall, 1992).

The proliferation of microglia may influence or be influenced by other physiological processes that take place in the developing CNS. The highest expression of PCNA by microglia coincides with or takes place immediately prior to the period of maximal dendritic growth and synapse formation (Zimmer, 1978; Uylings et al., 1990; Jacobson, 1991c) and to the period of macroglial proliferation, sprouting of brain capillaries (Jacobson, 1991b), and myelination (Baumann and Pham-Dinh, 2001). The reduction in the number of PCNA-positive microglia observed between P9 and P18 occurs in parallel with the terminal maturation of the cytoarchitecture of most CNS regions (Hebel and Stromberg, 1986) and the time point when the adult resting microglia become homogeneously distributed in the brain (Murabe and Sano, 1982; Perry et al., 1985; Dalmau et al., 1998a). In gray matter, microglia proliferated throughout development. However, at most ages, the massive proliferation of microglia did not result in a significant increase in cell density, presumably because of growth associated with brain morphogenesis. The rat cerebral cortex experiences rapid growth during the late prenatal period and postnatally from birth until about day 8, after which no notable changes in size occur (Uylings et al., 1990). Accordingly, despite the continuous microglial proliferation, the density of microglia in the cerebral cortex remained relatively constant but had increased significantly by P9 and reached the maximal density at P18. Therefore, microglial proliferation is able to compensate for the prominent growth of the cerebral cortex from E16 to the first postnatal week. Only from P9 to P18, when the growth declines, does proliferation result in a significant increase in microglial density. The same reasoning is plausible for Ammon's horn, in that its temporal pattern of growth (Bayer, 1980) is similar to that of the neocortex, and, similarly, the microglial density increased postnatally, reaching the highest values at P18. For the dentate gyrus, we observed a gradual but slow increase in microglial density from E18 to P9 and a subsequent significant decrease up to P18. Once again, the temporal changes in microglial density correlate well with morphogenetics, insofar as the growth rate of the dentate gyrus remains high from the second postnatal week (Bayer, 1980) compared with that in Ammon's horn. This rate has been assessed to be from 17% to 28% daily, which may partially explain the reduction in microglial cell density seen at P18. However, mechanisms other than proliferation and morphogenetics might also be relevant (Fig. 4). Microglial precursors recruited in white matter may migrate into the adjacent gray matter (Ling et al., 1980; Murabe and Sano, 1982; Navascués et al., 1996; Rezaie et al., 1997; Dalmau et al., 1998a). It has also been suggested that some microglial precursors in gray matter are derived from pial elements (Del Río Hortega, 1932; Boya et al., 1991; Sorokin et al., 1992; Navascués et al., 1996; Dalmau et al., 1997a, 1998a) or from hematogenous cells that extravasate through blood vessels in gray matter (Dalmau et al., 1997b); however, the specific contribution of these mechanisms is not known.

In contrast to gray matter, early prenatal white matter was characterized by the presence of abundant microglia (AM) and low microglial proliferation. In particular, the subcortical white matter on E18 showed a very low per-

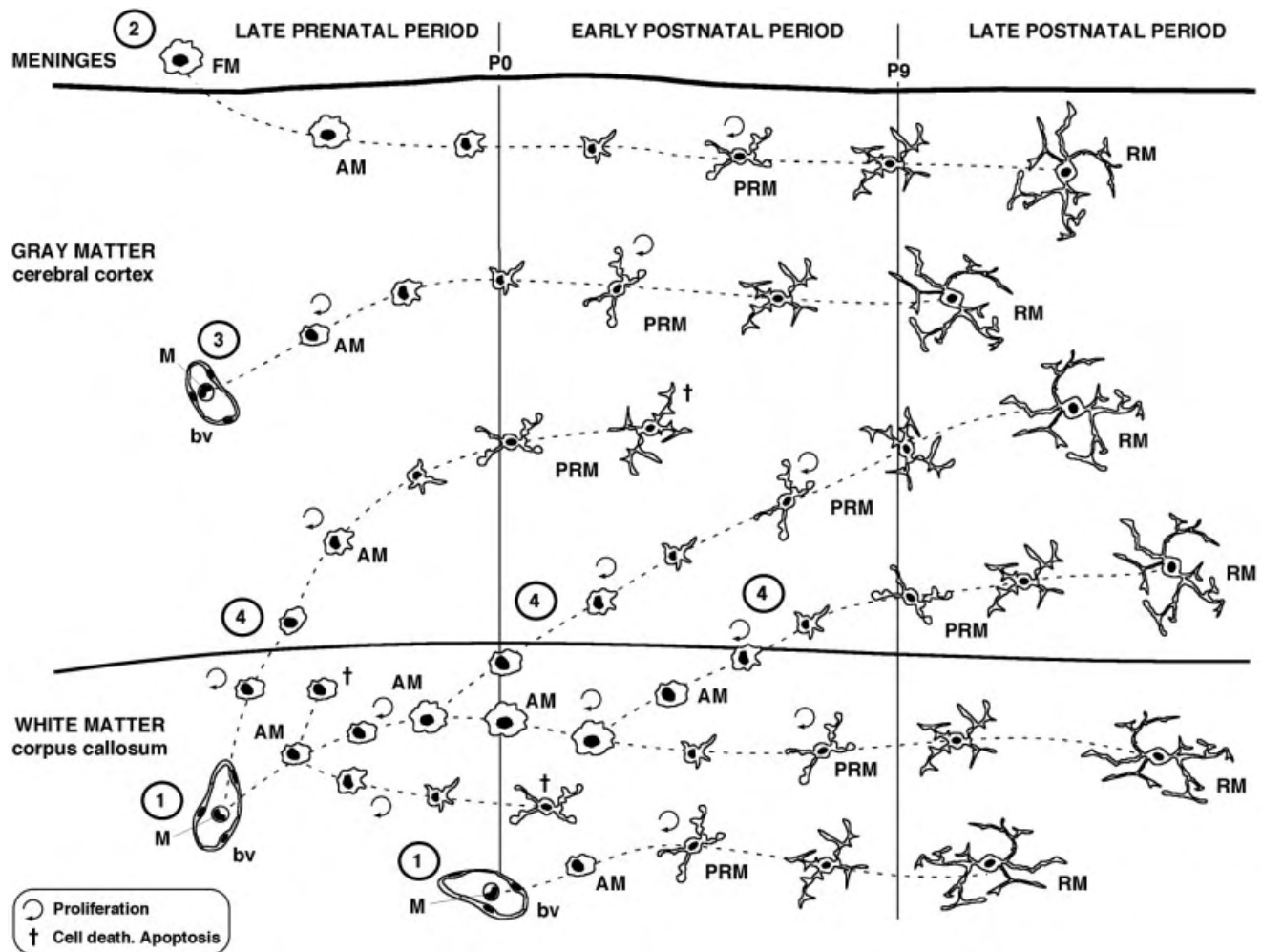


Fig. 4. Proposed scheme for microglial population growth in the developing brain. This scheme is based on the present study and our previous investigations of microglial ontogenesis (Dalmau et al., 1997a,b, 1998a,b). Two presumed main entry routes of microglial progenitors into the developing brain are illustrated. Although microglial cell progenitors of monocyte-like (M) nature may migrate into the brain through the parenchymal blood vessels of the developing white matter (1) by up-regulation of cell adhesion molecules such as the LFA-1 $\alpha$ /ICAM-1 system, microglial progenitors of fetal macrophage (FM) origin may be recruited into the developing gray matter from the surrounding meninges (2). However, the entry of monocyte-like cells (3) from the parenchymal vascular network in the gray matter cannot be discounted either. Apart from the fetal macrophage homing in the gray matter, recruitment of microglial precursors (4) from the neighboring white matter following a centrifugal migration pattern may

also participate in the microglial homing, as previously suggested from other studies (see Cuadros and Navascués, 1998). Similarly to the case for other cells in the nerve tissue, microglial proliferation of cell precursors previous to their differentiation into mature cells is also a common phenomenon occurring during normal brain development, as shown in the present investigation. Therefore, not only the entrance but also the cell division during both prenatal and postnatal periods are crucial for the establishment of normal mature microglial density. Finally, the observation of TUNEL- and caspase-3-positive microglia suggests that apoptosis is a physiological mechanism of microglial cell death in the developing CNS and may suggest the hypothesis of the existence of a transitory cell population with specific functions and a fate different from that of cells differentiating into resting microglia. AM, ameboid microglia; PRM, primitive ramified microglia; RM, resting microglia; bv, blood vessels.

centage (about 3%) of proliferating microglia, although the density of microglia was extremely high. This agrees with previous studies showing that this brain region is rapidly colonized by newly recruited AM (mostly from E18 in the rat), which may arise from blood monocytes that extravasate and disseminate through the developing white matter (Ling, 1979; Perry et al., 1985; Ashwell, 1991; Boya et al., 1991; Dalmau et al., 1997b, 1998a). On this basis, entrance and not proliferation seems to be the major source of microglia in white matter at the earliest stages. From this time, there was a gradual increase in the per-

centage of proliferating microglia during the prenatal and postnatal periods, reaching the maximum on day P9 (95% and 92% in the subcortical white matter and the fimbria, respectively). Therefore, both recruitment and proliferation play a role in the establishment of the pool of microglial precursors in white matter (Fig. 4). In contrast to that of monocyte recruitment, the contribution of proliferation to the microglial cell population gradually increases with time. Morphogenetic changes in volume, migration of microglia, and cell death might also contribute to variations in the microglial density during the formation of the

white matter (Fig. 4). Some microglial precursors initially recruited in white matter may migrate into the gray matter. This phenomenon may occur, in the late embryonic and early postnatal periods, and presumably counteracts, in terms of microglial density, the effect of extravasation and proliferation (Fig. 4). Nevertheless, its specific contribution cannot be evaluated, because the precise temporal pattern and percentage of microglia engaged in this migratory process are presently unknown. Another factor is that the white matter experiences considerable growth during development as a result of the progressive increase in axon diameter and myelination. Myelin deposition and assembly in the rat brain begins postnatally at about 10–12 days (Morell et al., 1989), when axons have acquired an adequate diameter. Thus, the growth in diameter of axons could influence cell density throughout development, whereas myelination likely contributes to the final decrease in microglial density observed from P9 to P18. In this way, the presence of significant numbers of proliferating microglia in white matter at P18 (32–33% of microglial cells) indicates that microglial expansion is still needed, in accordance with the observation that myelination is still incomplete at this age (Raine, 1984; Baumann and Pham-Dinh, 2001).

### Microglial apoptosis

By using TUNEL histochemistry and caspase-3 immunohistochemistry, we have demonstrated the existence of apoptotic microglial cells in the developing rat brain. A few previous studies have also supported the possibility of microglial cell death in the developing brain. In an autoradiographic study in the developing corpus callosum, Imamoto and Leblond (1978) suggested that one-third of amoeboid microglia are transformed into ramified microglia during the first 3 weeks of life, while the other two-thirds degenerate. In a morphometric study of the transformation of amoeboid microglia into ramified microglia in the rat corpus callosum, Wu and collaborators (1992) also suggested that the reduction of microglial density after P13 was due to cell death. Finally, more recently, de Louw and collaborators (2002) identified TUNEL-positive microglia in the rat spinal cord at P2, P5, and P8 and reported that 18% of degenerating cells could be identified as microglia/macrophages. Thus, similarly to what occurs with neurons, astrocytes, and oligodendrocytes, it seems plausible that the balance between cell proliferation and death could also regulate the number of cells from the microglial lineage during development. However, in the present study using double-labeling techniques and two sets of markers generally used to detect cells undergoing apoptosis, we report that microglial apoptosis has a low incidence and is restricted mainly to some AM encountered in white matter areas mostly during the late embryonic period and some PRM in gray matter areas mostly in the postnatal period from P6 to P9. Because cell death occurs only locally at certain ages and at low levels, when the density of microglia is high and before the terminal differentiation of microglial precursors into mature microglia, we may deduce that apoptosis does not play a major role in regulating microglial density during rat brain development. Differences in data from previous reports may be related either to regional differences or to differences in the time points analyzed.

Interestingly, in comparing the microglial cells in the different brain regions with proliferation ratio of micro-

glial cell population, there is only a modest gain in the microglial cell density and even a decline in certain regions, such as the dentate gyrus, from P9 to P18. This observation could be explained, as hypothesized in the present study, either by the dramatic changes of volume expansion during CNS development or by death of cells of the microglial lineage through an apoptotic mechanism. In addition, as suggested for some experimental models, microglial cells may migrate out of the brain along the vascular network (Sørensen et al., 1996).

### Phagocytosis of apoptotic cells by microglia

Microglia are resident CNS macrophages and have the potential to become phagocytes when activated after injury. In the developing CNS, cells of the microglial lineage have also been involved in the removal of dead cells (Ashwell, 1990, 1991; Ferrer et al., 1990; Ellison and Vellis, 1995; Moujahid et al., 1996) and exuberant axonal projections (Innocenti et al., 1983a,b). In this study, we found that degenerating cells undergoing apoptosis were frequently engulfed by microglial cells. The quantitative analysis showed that a high percentage (more than 70% in most areas, except for a few ages in certain brain regions) of TUNEL-positive cells was partially or totally surrounded by microglia. Interestingly, not only are AM active phagocytes in the immature brain (for reviews see Ashwell and Bobryshev, 1996; Perry, 2001; Streit, 2001) but also PRM are involved in the removal of apoptotic cells. These data are in agreement with the observation of Murabe and Sano (1982) that microglial cells during the postnatal development of the rat brain contain numerous phagosomes in their cytoplasm. Although cells other than microglia, such as Müller cells in the developing retina (Egensperger et al., 1996; Marin-Teva et al., 1999b) or astrocytes in mixed-glia cell cultures from neonatal brains (Tansey and Cammer, 1998), have been reported to exhibit phagocytic capacity, our findings tend further to support the view that microglia are the main phagocytes in the developing brain.

The presence of dead cells and cell debris in the damaged tissue is considered to be a major signal for microglial activation and proliferation in the injured CNS (Miyake and Kitamura, 1991; Giordana et al., 1994; Vela et al., 2002). However, on the basis on the present study (Tables 1, 2), a direct cause-and-effect correspondence between cell death and microglial proliferation cannot be established for the developing rat brain. A similar conclusion was reached for the developing mouse cerebellum (Ashwell, 1990). Therefore, it seems clear that, although degeneration may act as a local stimulus for the proliferation of microglia, the presence of degenerating cells per se does not explain the sustained proliferation and regional distribution of microglia during development. Soluble proteins acting as mitogens for microglia have been detected during CNS formation (Guilian and Ingeman, 1988; Guilian et al., 1991; Elkabes et al., 1996). The increase in the density of proliferating microglia from E18 to P9 correlates with the presence of two specific microglial mitogens, MM1 and MM2 (Guilian et al., 1991). The colony-stimulating factors (CSFs; Raivich et al., 1994a,b; Blevins and Fedoroff, 1995), particularly CSF-1, has been demonstrated early in the immature mouse brain in a region-specific manner (Pollard, 1997) and persisted throughout development (Théry et al., 1990; Mehler and Kessler, 1994). Altogether, both signals from dying cells and solu-

ble factors may be responsible for promoting the sustained proliferation of microglia during the formation of the CNS.

## CONCLUSIONS

The present study shows that proliferation represents a major source of microglia in the developing brain. On this basis, not only entrance but also proliferation during both pre- and postnatal development appear to be crucial for the establishment of the normal mature microglial cell population. Only once the brain has matured and no dramatic change in volume occurs does the cell division of microglia result in the increased density values observed in the normal adult brain. Thus, proliferation serves to maintain a relatively constant density of microglia during the period when the brain undergoes its maximal volume expansion from the late prenatal period to the second postnatal week. Apoptosis may also regulate the number of microglia during development by acting locally at certain ages and in certain locations, but it seems less crucial for the establishment of the final microglial population. Finally, although microglia are the main phagocyte responsible for the elimination of dying cells during development, the presence of degenerating cells does not explain per se the proliferation pattern and the regional distribution of microglial cells during development.

## ACKNOWLEDGMENTS

The authors acknowledge the excellent technical assistance of Miguel A. Martil and Anna Garrit.

## LITERATURE CITED

- Acarin L, Vela JM, González B, Castellano B. 1994. Demonstration of poly-N-acetyl lactosamine residues in amoeboid and ramified microglial cells in rat brain by tomato lectin binding. *J Histochem Cytochem* 42:1033-1041.
- Adamson DC, Dawson TM, Zink MC, Clements JE, Dawson VL. 1996. Neurovirulent simian immunodeficiency virus infection induces neuronal, endothelial, and glial apoptosis. *Mol Med* 4:417-428.
- Alliot F, Godin I, Pessac B. 1999. Microglia derive from progenitors, originating from yolk sac, and which proliferate in the brain. *Brain Res Dev Brain Res* 117:145-152.
- Altman J, Bayer SA. 1995. Atlas of prenatal rat brain development. Boca Raton, FL: CRC Press.
- Ashwell K. 1990. Microglia and cell death in the developing mouse cerebellum. *Brain Res Dev Brain Res* 55:219-230.
- Ashwell K. 1991. The distribution of microglial and cell death in the fetal rat forebrain. *Brain Res Dev Brain Res* 58:1-12.
- Ashwell KWS, Bobryshev YV. 1996. The developmental role of microglia. In: Ling EA, Tan CK, Tan CBC, editors. Topical issues in microglia research. Singapore: Singapore Neuroscience Association. p 65-82.
- Avanzi GC, Porcu P, Brizzi MF, Ghigo D, Bosia A, Pegoraro L. 1991. Interleukin-3-dependent proliferation of the human MO-7e cell line is supported by discrete activation of late G<sub>1</sub> genes. *Cancer Res* 51:1741-1743.
- Bancroft JD, Stevens A. 1996. Mounting media. In: Bancroft JD, Stevens A, editors. Theory and practice of histological techniques. New York: Churchill Livingstone. p 735.
- Baumann N, Pham-Dinh D. 2001. Biology of oligodendrocyte and myelin in the mammalian central nervous system. *Physiol Rev* 81:871-927.
- Bayer SA. 1980. Development of the hippocampal region in the rat. II. Morphogenesis during embryonic and early postnatal life. *J Comp Neurol* 190:115-134.
- Blevins G, Fedoroff S. 1995. Microglia in colony-stimulating factor 1-deficient op/op mice. *J Neurosci Res* 40:535-544.
- Boya J, Calvo JL, Carbonell AL, Borregon A. 1991. A lectin histochemistry study on the development of rat microglial cells. *J Anat* 175:229-236.
- Cowan WM, Fawcett JW, O'Leary DDM. 1984. Regressive events in neurogenesis. *Science* 225:1258-1265.
- Cuadros MA, Navascués J. 1998. The origin and differentiation of microglial cells during development. *Prog Neurobiol* 56:173-189.
- Cuadros MA, Navascués J. 2001. Early origin and colonization of the developing central nervous system by microglial precursors. In: Castellano B, Nieto-Sampedro M, editors. Glial cell function. Amsterdam: Elsevier. p 51-59.
- Dalmau I. 1998. Las células de microglía en el cerebro de la rata en desarrollo. Doctoral thesis. Bellaterra: Publicacions de la Universitat Autònoma de Barcelona.
- Dalmau I, Finsen B, Tønder N, Zimmer J, González B, Castellano B. 1997a. Development of microglia in the prenatal rat hippocampus. *J Comp Neurol* 377:70-84.
- Dalmau I, Vela JM, González B, Castellano B. 1997b. Expression of LFA-1 $\alpha$  and ICAM-1 in the developing rat brain: a potential mechanism for the recruitment of microglial cell precursors. *Brain Res Dev Brain Res* 103:163-170.
- Dalmau I, Vela JM, González B, Castellano B. 1998a. Expression of purine metabolism-related enzymes by microglial cells in the developing rat brain. *J Comp Neurol* 398:333-346.
- Dalmau I, Finsen B, Zimmer J, González B, Castellano B. 1998b. Development of microglia in the postnatal rat hippocampus. *Hippocampus* 8:458-474.
- De Louw AJA, Van de Berg WDJ, De Vente J, Blanco CE, Gavilanes AWD, Steinbusch HPJ, Steinbusch HWM, Troost J, Vles JSH. 2002. Developmental apoptosis in the spinal cord white matter in neonatal rats. *Glia* 37:89-91.
- Del Río Hortega P. 1932. Microglia. In: Penfield W, editor. Cytology and cellular pathology of the nervous system, vol 2. New York: Paul B. Hoeber. p 481-534.
- D'Mello SR. 1998. Molecular regulation of neuronal apoptosis. *Curr Top Dev Biol* 39:187-213.
- Egensperger R, Maslim J, Bisti S, Hollander H, Stone J. 1996. Fate of DNA from retinal cells dying during development: uptake by microglia and macroglia (Müller cells). *Brain Res Dev Brain Res* 97:1-8.
- Elkabes S, DiCicco-Bloom EM, Black IB. 1996. Brain microglia/macrophages express neurotrophins that selectively regulate microglial proliferation and function. *J Neurosci* 16:2508-2521.
- Ellison JA, de Vellis J. 1995. Amoeboid microglia expressing GD3 ganglioside are concentrated in regions of oligodendrogenesis during development of the rat corpus callosum. *Glia* 14:123-132.
- Fedoroff S, Zhai R, Novak JP. 1997. Microglia and astroglia have a common progenitor cell. *J Neurosci Res* 50:477-486.
- Ferrer I, Bernet E, Soriano E, Del Río JA, Fonseca M. 1990. Naturally occurring cell death in the cerebral cortex of the rat and removal of dead cells by transitory phagocytes. *Neuroscience* 39:451-458.
- Ferrer I, Tortosa A, Blanco R, Martín F, Serrano T, Planas A, Macaya A. 1994. Naturally occurring cell death in the developing cerebral cortex of the rat. Evidence of apoptosis-associated internucleosomal DNA fragmentation. *Neurosci Lett* 182:77-79.
- Frei K, Bodmer S, Schwerdel C, Fontana A. 1986. Astrocyte-derived interleukin 3 as a growth factor for microglial cells and peritoneal macrophages. *J Immunol* 137:3521-3527.
- Gadbois DM, Peterson S, Bradbury EM, Lehnert BE. 1995. Cdk4/Cyclin D1/PCNA complexes during staurosporine-induced G<sub>1</sub> arrest and G<sub>0</sub> arrest of human fibroblasts. *Exp Cell Res* 220:220-225.
- Ganter S, Northoff H, Männel D, Gebicke-Härter PJ. 1992. Growth control of cultured microglia. *J Neurosci Res* 33:218-230.
- Gavrieli Y, Sherman Y, Ben-Sasson SA. 1992. Identification of programmed cell death in situ via specific labeling of nuclear DNA fragmentation. *J Cell Biol* 119:493-501.
- Giordana MT, Attanasio A, Cavalla P, Migheli A, Vighiani MC, Schiffer D. 1994. Reactive cell proliferation and microglia following injury to the rat brain. *Neuropathol Appl Neurobiol* 20:163-174.
- Giulian D, Ingeman J. 1988. Colony stimulating factors as activators of amoeboid microglia. *J Neurosci* 8:4701-4712.
- Giulian D, Johnson B, Krebs JF, George JK, Tapscott M. 1991. Microglial mitogens are produced in the developing and injured mammalian brain. *J Cell Biol* 112:323-333.
- Gown AM, Willingham MC. 2002. Improved detection of apoptotic cells in

- archival paraffin sections: immunocytochemistry using antibodies to cleaved caspase 3. *J Histochem Cytochem* 50:449–454.
- Hao C, Richardson A, Fedoroff S. 1991. Macrophage-like cells originate from neuroepithelium in culture: characterization and properties of the macrophage-like cells. *Int J Dev Neurosci* 9:1–14.
- Hebel R, Stromberg MW. 1986. Anatomy and embryology of the laboratory rat, nervous system. Wörthsee: BioMed Verlag. p 124–217.
- Imamoto K, Leblond CP. 1978. Radioautographic investigation of gliogenesis in the corpus callosum of young rats. *J Comp Neurol* 180:139–164.
- Innocenti GM, Koppel H, Clarke S. 1983a. Transitory macrophages in the white matter of the developing visual cortex. I. Light and electron microscopic characteristics and distribution. *Brain Res Dev Brain Res* 11:39–53.
- Innocenti GM, Clarke S, Koppel H. 1983b. Transitory macrophages in the white matter of the developing visual cortex. II. Development and relations with axonal pathways. *Brain Res Dev Brain Res* 11:55–66.
- Jacobson M. 1991a. The germinal cell, histogenesis, and lineages of nerve cells. In: Jacobson M, editor. *Developmental neurobiology*. New York: Plenum Press. p 41–94.
- Jacobson M. 1991b. Neuroglial ontogeny. In: Jacobson M, editor. *Developmental neurobiology*. New York: Plenum Press. p 95–139.
- Jacobson M. 1991c. Formation of dendrites and development of synaptic connections. In: Jacobson M, editor. *Developmental neurobiology*. New York: Plenum Press. p 223–279.
- Kaur C, Ling EA, Wong WC. 1989. Development of the various glial cell types in the cerebral cortex of postnatal rats. *Acta Anat* 136:204–210.
- Kaur C, Hao AJ, Wu CH, Ling EA. 2001. Origin of microglia. *Microsc Res Tech* 54:2–9.
- Kelman Z. 1997. PCNA: structure, functions and interactions. *Oncogene* 14:629–640.
- Kloss CUA, Kreutzberg GW, Raivich G. 1997. Proliferation of ramified microglia on an astrocyte monolayer: characterization of stimulatory and inhibitory cytokines. *J Neurosci Res* 49:248–254.
- Kreutzberg GW. 1996. Microglia: a sensor for pathological events in the CNS. *Trends Neurosci* 19:312–318.
- Krueger BK, Burne JF, Raff MC. 1995. Evidence for large-scale astrocyte death in the developing cerebellum. *J Neurosci* 15:3366–3374.
- Kurki P, Ogata K, Tan EM. 1988. Monoclonal antibodies to proliferating cell nuclear antigen (PCNA)/cyclin as probes for proliferating cells by immunofluorescence microscopy and flow cytometry. *J Immunol Methods* 109:49–59.
- Lassmann H, Bancher C, Breitschopf H, Wegiel J, Bobinski M, Jellinger K, Wisniewski HM. 1995. Cell death in Alzheimer's disease evaluated by DNA fragmentation in situ. *Acta Neuropathol* 89:35–41.
- Ling EA. 1979. Transformation of monocytes into amoeboid microglia and into microglia in the corpus callosum of postnatal rats, as shown by labelling monocytes by carbon particles. *J Anat* 129:847–858.
- Ling EA, Penney D, Leblond CP. 1980. Use of carbon labelling to demonstrate the role of blood monocytes as precursors of the "amoeboid cells" present in the corpus callosum of postnatal rats. *J Comp Neurol* 193:631–657.
- Liuzzi GM, Santacrose MP, Peumans WJ, Van Damme EJ, Dubois B, Opdenakker G, Riccio P. 1999. Regulation of gelatinases in microglia and astrocyte cell cultures by plant lectins. *Glia* 27:53–61.
- Mander TH, Morris JF. 1996. Development of microglia and macrophages in the postnatal rat pituitary. *Cell Tissue Res* 286:347–355.
- Marín-Teva JL, Almendros A, Calvente R, Cuadros MA, Navascues J. 1999a. Proliferation of actively migrating amoeboid microglia in the developing quail retina. *Anat Embryol* 200:289–300.
- Marín-Teva JL, Cuadros MA, Calvente R, Almendros A, Navascues J. 1999b. Naturally occurring cell death and migration of microglial precursors in the quail retina during normal development. *J Comp Neurol* 412:255–275.
- McCormick D, Hall PA. 1992. The complexities of proliferating cell nuclear antigen. *Histopathology* 21:591–594.
- Mehler MF, Kessler JA. 1994. Growth factor regulation of neuronal development. *Dev Neurosci* 16:180–195.
- Milligan CE, Cunningham TJ, Levitt P. 1991. Differential immunohistochemical markers reveal the normal distribution of brain macrophages and microglia in the developing rat brain. *J Comp Neurol* 314:125–135.
- Miyake T, Kitamura T. 1991. Proliferation of microglia in the injured cerebral cortex of mice as studied by thiamine pyrophosphatase histochemistry combined with <sup>3</sup>H-thymidine autoradiography. *Acta Histochem Cytochem* 24:457–463.
- Morell P, Quarles RH, Norton WT. 1989. Formation, structure, and biochemistry of myelin. In: Siegel GJ, Agranoff BW, Alberts RW, Molinoff PB, editors. *Basic neurochemistry*. New York: Raven Press. p 109–136.
- Moujahid A, Navascues J, Marín-Teva JL, Cuadros MA. 1996. Macrophages during avian optic nerve development: relationship to cell death and differentiation into microglia. *Anat Embryol* 193:131–144.
- Murabe Y, Sano Y. 1982. Morphological studies on neuroglia. VI. Postnatal development of microglial cells. *Cell Tissue Res* 225:469–485.
- Navascues J, Cuadros MA, Almendros A. 1996. Development of microglia: evidence from studies in the avian central nervous system. In: Ling EA, Tan CK, Tan CBC, editors. *Topical issues in microglial research*. Singapore: Singapore Neuroscience Association. p 43–64.
- Nguyen KB, McCombe PA, Pender MP. 1994. Macrophage apoptosis in the central nervous system in experimental autoimmune encephalomyelitis. *J Autoimmun* 7:145–152.
- Ogata T, Shubert P. 1996. Programmed cell death in rat microglia is controlled by extracellular adenosine. *Neurosci Lett* 218:91–94.
- Oppenheim RW. 1991. Cell death during development of the nervous system. *Annu Rev Neurosci* 14:453–501.
- Perry VH. 2001. Microglia in the developing and mature central nervous system. In: Jessen KR, Richardson WD, editors. *Glial cell development*. New York: Oxford University Press. p 75–90.
- Perry VH, Hume DA, Gordon S. 1985. Immunohistochemical localization of macrophages and microglia in the adult and developing mouse brain. *Neuroscience* 15:313–326.
- Pollard JW. 1997. Role of colony-stimulating factor-1 in reproduction and development. *Mol Reprod Dev* 46:54–60.
- Raff MC, Barres BA, Burne JF, Coles HS, Ishizaki Y, Jacobson MD. 1993. Programmed cell death and the control of cell survival: lessons from the nervous system. *Science* 262:695–700.
- Raine CS. 1984. Morphology of myelin and myelination. In: Morell P, editor. *Myelin*. New York: Plenum Press. p 1–50.
- Raivich G, Moreno-Flores MT, Moller JC, Kreutzberg GW. 1994a. Inhibition of post-traumatic microglial proliferation in a genetic model of macrophage colony-stimulating factor deficiency in the mouse. *Eur J Neurosci* 6:1615–1618.
- Raivich G, Moreno-Flores MT, Moller JC, Kreutzberg GW. 1994b. Regulation of microglial proliferation: colony-stimulating factors and their receptors. *Neuropathol Appl Neurobiol* 2:209–211.
- Rezaie P, Cairns NJ, Male DK. 1997. Expression of adhesion molecules on human fetal cerebral vessels: relationship to microglial colonisation during development. *Brain Res Dev Brain Res* 104:175–189.
- Ross ME. 1996. Cell division and the nervous system: regulating the cycle from neural differentiation to death. *Trends Neurosci* 19:62–68.
- Roth KA, D'Sa C. 2001. Apoptosis and brain development. *Ment Retard Dev Disabil Res Rev* 7:261–266.
- Sommer L, Rao M. 2002. Neural stem cells and regulation of cell number. *Prog Neurobiol* 66:1–18.
- Sørensen JC, Dalmau I, Zimmer J, Finsen B. 1996. Microglial reactions to retrograde degeneration of tracer-identified thalamic neurons after frontal sensorimotor cortex lesions in adult rats. *Exp Brain Res* 112:203–212.
- Soriano E, del Río JA, Auladell C. 1993. Characterization of the phenotype and birthdates of pyknotic dead cells in the nervous system by a combination of DNA staining and immunohistochemistry for 5'-bromodeoxyuridine and neural antigens. *J Histochem Cytochem* 41:819–827.
- Sorokin SP, Hoyt RF Jr, Blunt DG, McNelly NA. 1992. Macrophage development: II. Early ontogeny of macrophage populations in brain, liver, and lungs of rat embryos as revealed by a lectin marker. *Anat Rec* 232:527–550.
- Streit WJ. 2001. Microglia and macrophages in the developing CNS. *Neurotoxicology* 22:619–624.
- Streit WJ, Walter SA, Pennell NA. 1999. Reactive microgliosis. *Prog Neurobiol* 57:563–581.
- Suzumura A, Sawada M, Yamamoto H, Marunouchi T. 1990. Effects of colony stimulating factors on isolated microglia in vitro. *J Neuroimmunol* 30:237–244.
- Tansey FA, Cammer W. 1998. Differential uptake of dextran beads by astrocytes, macrophages and oligodendrocytes in mixed glial-cell cultures from brains of neonatal rats. *Neurosci Lett* 248:159–162.
- Théry C, Hetier E, Evrard C, Mallat M. 1990. Expression of macrophage colony-stimulating factor gene in the mouse brain during development. *J Neurosci Res* 26:129–133.

- Tomozawa Y, Inoue T, Takahashi M, Adachi M, Satoh M. 1996. Apoptosis of cultured microglia by the deprivation of macrophage colony-stimulating factor. *Neurosci Res* 25:7–15.
- Uylings HBM, Van Eden CG, Parnavelas JG, Kalsbeek A. 1990. The prenatal and postnatal development of rat cerebral cortex. In: Kolb B, Tees RC, editors. *The cerebral cortex of rat*. Cambridge, MA: MIT Press. p 35–76.
- Vela JM, Dalmau I, González B, Castellano B. 1996. The microglial reaction in spinal cords of jimpy mice is related to apoptotic oligodendrocytes. *Brain Res* 712:134–142.
- Vela JM, Dalmau I, González B, Castellano B. 1997. Abnormal expression of PCNA in the spinal cord of the hypomyelinated jimpy mutant mice. *Brain Res* 747:130–139.
- Vela JM, Yáñez A, González B, Castellano B. 2002. Time course of proliferation and elimination of microglia/macrophages in different neurodegenerative conditions. *J Neurotrauma* 19:1503–1520.
- Wu CH, Wen CY, Shieh JY, Ling EA. 1992. A quantitative and morphometric study of the transformation of amoeboid microglia into ramified microglia in the developing corpus callosum in rats. *J Anat* 181:4423–4430.
- Yang MS, Park EJ, Sohn S, Kwon HJ, Shin WH, Pyo HK, Jin B, Choi KS, Jou I, Joe EH. 2002. Interleukin-13 and -4 induce death of activated microglia. *Glia* 38:273–280.
- Zhu BC-R, Laine RA. 1989. Purification of acetyllactosamine-specific tomato lectin by erythroglucan-sepharose affinity chromatography. *Prep Biochem* 19:341–350.
- Zimmer J. 1978. Development of the hippocampus and fascia dentata. Morphological and histochemical aspects. In: Corner MA, Baker RE, Van de Pol NE, Swaab DF. editors, *Progress in brain research: maturation of the nervous system*. Amsterdam: Elsevier North-Holland Biochemical Press. p 171–190.
- Zölzer F, Streffer C, Pelzer T. 1994. A comparison of different methods to determine cell proliferation by flow cytometry. *Cell Prolif* 27:685–694.